CoNF-900914--13

UCRL-JC-103491
PREPRINT

A CHARACTERIZATION OF INTERNAL-SN NB_3SN SUPERCONDUCTORS FOR USE IN THE PROOF OF PRINCIPLES (PoP) COIL

L. T. Summers
A. R. Duenas
C. E. Karlsen
G. M. Ozeryansky
E. Gregory

This paper was prepared for submittal to the
1990 Applied Superconductivity Conference,
Snowmass Village, CO, 9/24-28/90

Received by OSTI
NOV 05 1990

September 21, 1990

Lawrence Livermore National Laboratory

A CHARACTERIZATION OF INTERNAL-SN NB3SN SUPERCONDUCTORS FOR USE IN THE PROOF OF PRINCIPLES (POP) COIL

L.T. Summers, A.R. Duenas, and C.E. Karlsen
Lawrence Livermore National Laboratory
P.O. Box 5511, L-643
Livermore, CA 94550

UCRL-JC--103491

DE91 001743

G.M. Ozeryansky and E. Gregory
Intermagnetics General Corporation
1875 Thomaston Ave
Waterbury , CT 06704

Abstract

High performance Ti-alloyed internal-Sn superconductors have been selected for use in the the Proof of Principles (PoP) coil, a 1.0 m o.d., 0.4 m i.d., solenoid designed to produce fields up to 15 T. The PoP coil, which will use forced-flow Cable-In-Conduit Conductors (CICC), will operate at 4.2 K and moderate levels of conductor strain. Here we report the results of detailed characterizations of two proposed PoP coil Nb_3Sn 19 subelement superconducting wires of differing topology. We have investigated the critical current as a function of applied field, and applied strain. The wires were found to have excellent high field properties, providing a high performance margin for the proposed PoP coil. The field and strain dependence of J_c have been found to compare favorably with predictions from a wire performance model recently developed for Nb_3Sn superconductors.

Introduction

The Proof of Principles (PoP) coil is designed as a 1.0 m o.d., 0.4 m i.d. solenoid for use in demonstrating the engineering design principles assumed for large magnets proposed for magnetic fusion energy machines such as the International Thermonuclear Experimental Reactor (ITER). The PoP coil is capable of producing a field of 15 T when operated in the 8 T backing field provided by the 2.0 m solenoid located at the LLNL High Field Test Facility (HFTF).

Two grades of forced-flow conductors will be used for PoP, the low field grade consisting of a $5^2 \times 3$ cable enclosed in a square stainless steel conduit measuring 7.47 mm flat to flat externally and having a wall thickness of 0.6 mm. The high field grade will have a 5^3 cable and be enclosed in a conduit measuring 9.29 mm externally with a 0.6 mm wall thickness. The operating current of both grades is 5 kA.

Internal-Sn, Ti alloyed multifilamentary superconductors have been selected for use in the PoP coil. At the time of their specification the conductors for PoP represented the state-of-the-art of superconductor manufacture, a level of technology that is not only suitable for PoP but possibly also for magnet systems in ITER.

Experimental Procedure

The wire selected for the PoP conductor is an 19 subelement, internal-tin, Nb_3Sn superconducting wire

Manuscript received September 24, 1990

Experimental Procedure

The wire selected for the PoP conductor is an 19 subelement, internal-tin, Nb_3Sn superconducting wire produced by Intermagnetics General Corporation. This wire was produced in two variants with slightly different topologies. The first variant contains a copper layer measuring approximately 25 μm thick immediately under the diffusion barrier. This layer, referred to as under-barrier copper, is beneficial in increasing transverse resistivity, increasing subelement uniformity, and possibly increasing drawability. The second variant of this wire was produced without under-barrier copper to achieve higher critical currents. The details of the wire construction appear in Table 1. For simplicity the wires with and without under-barrier are referred to as "with UBC" and "w/o UBC" respectively. Note that the wires are similar in all respects except filament size and the inclusion of under-barrier copper. Photomicrographs of the unreacted wires with and without under-barrier appear in Figure 1 a and b respectively.

Table 1. Construction of Internal-tin wires used in this study.

	with UBC	w/o UBC
Wire Diameter	0.817 mm	0.817 mm
Cu Stabilizer	46.5%	46.5%
Nb Diffusion Barrier (of non-Cu area)	8.5%	8.5%
Non-Cu	53.5%	53.5%
No. Filaments	4902	4902
Filament Diameter	3.5 μm	3.7 μm
Subelement No.	19	19
Ti addition	1.2%	1.2%

Test specimens measuring 450 mm in length were heat treated in flowing argon according to the following schedule; 200°C/24h + 340°C/48h + 660°C/72h + 725°C/12h. No attempt was made to investigate optimal heat treatment schedules. The samples were then mounted in a critical current vs. strain test apparatus and tested at 4.2 K in a 15 T split bore solenoid. Details of the test apparatus are described elsewhere.[1,2] The gage length between specimen grips was 307 mm. The force applied to the specimen was measured directly with a load cell. Strain in the specimen was calculated from cross head displacement with an accounting for compliance in the load train.

For determination of critical current, sample voltage was measured over a 2 cm length of the wire centered at the

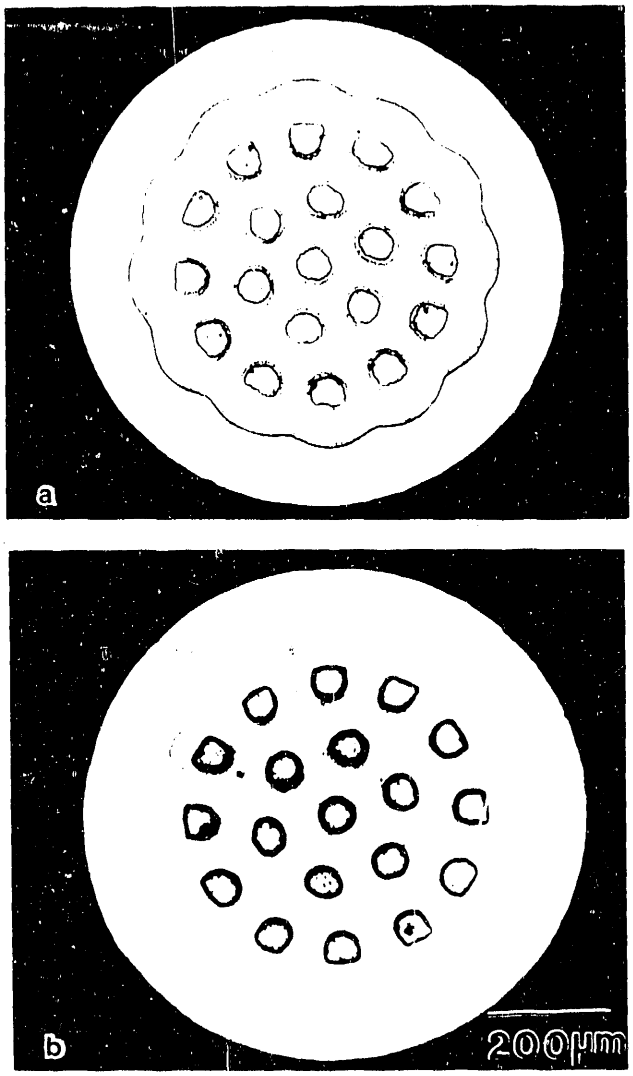

Figure 1. Photomicrographs of unreacted PoP coil wires, with under-barrier copper (a) and without under-barrier copper (b). The under-barrier copper (photograph a) is the thin layer of copper between the diffusion barrier and the outer row of subelements.

magnet bore. Critical current was measured using a resistance criteria of $5 \times 10^{-13}\ \Omega \cdot \mathrm{m}$. For purposes of J_c vs. ε testing, sample strain was adjusted using displacement control.

Theoretical calculation of the critical current of the sample wires was performed using a model developed at LLNL and based on previous work of Hampshire, et al. and Ekin.[3,4] The model allows prediction of critical current density in Nb_3Sn superconductors as a function of field, temperature, longitudinal strain, and radiation damage. Here we have used a simplified version of this equation that assumes a linear fit to the Ginzburg-Landau (κ) coefficient vs temperature and neglects the radiation dependent terms.

$$J_c(B,T,\varepsilon) \propto C\left[B_{c2}(T,\varepsilon)\right]^{-1/2}(1-t^2)^2\, b^{-1/2}(1-b)^2 \qquad (1)$$

where: $t = \dfrac{T}{T_{c0}(\varepsilon)}$

$b = \dfrac{B}{B_{c2}(T,\varepsilon)}$

C = Pinning/geometry factor accounting for fraction of Nb_3Sn and effectiveness of pinning sites.

$$B_{c2}(T,\varepsilon) = B_{c20}(\varepsilon)\left[1-\left(\frac{T}{T_{c0}(\varepsilon)}\right)^2\right]\left[1-\frac{1}{3}\left(\frac{T}{T_{c0}(\varepsilon)}\right)\right] \qquad (2)$$

where:

$B_{c20}(\varepsilon) = B_{c20m}(1 - a|\varepsilon|^u)$

$T_{c0}(\varepsilon) = T_{c0m}(1 - a|\varepsilon|^u)^{1/w}$

Details of the model are presented elsewhere.[5]

Application of the model requires assumptions of the critical temperature at zero intrinsic strain and zero field (T_{c0m}) and the upper critical field at zero intrinsic strain and zero temperature (B_{c20m}). For the purposes of this calculation the zero temperature critical field at zero intrinsic strain was fixed at 18.3 K. This is a reasonable assumption and is close to values used by Ekin to fit I_c vs strain data in Nb_3Sn wires.[4] B_{c20m} and the pinning/geometry factor (C) were varied to obtain the best fit to the data. It was assumed that B_{c20m} and T_{c0m} was the same for the two wire topologies and only the pinning/geometry factor was allowed to vary.

Results

A typical 4 K stress-strain curve is shown in Figure 2. The mechanical properties of both wires (w/ UBC and w/o UBC) are nearly identical. The 0.2% offset yield strengths are approximately 205 MPa and the tensile strengths are about 640 MPa. Separate mechanical tests have shown fracture to occur at about 1%.

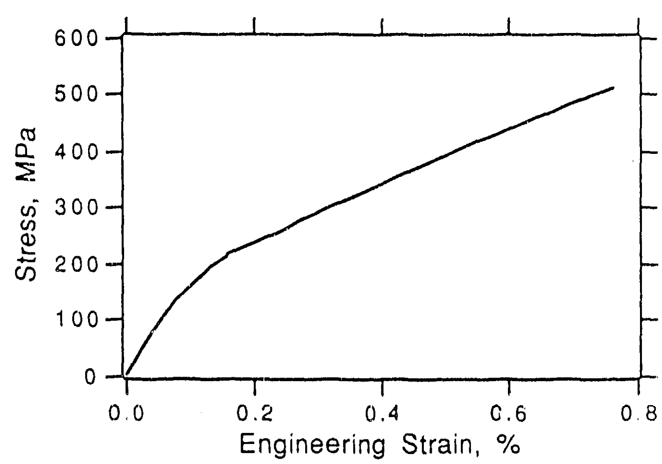

Figure 2. Typical 4 K stress-strain curve for the proposed PoP coil wires. This data was obtained during J_c vs. ε evaluation and the test was terminated at low I_c values and not at specimen fracture. Fracture observed in separate mechanical tests occurs at about 1% strain.

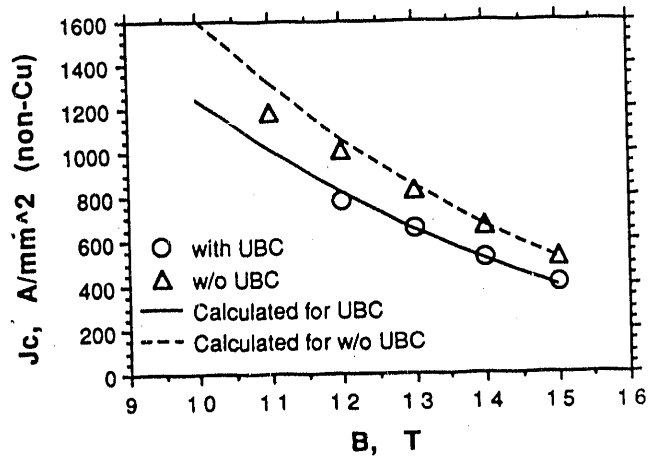

Figure 3. Jc as a function of B for both wires. Also plotted are values of Jc vs B calculated using Eq. 1.

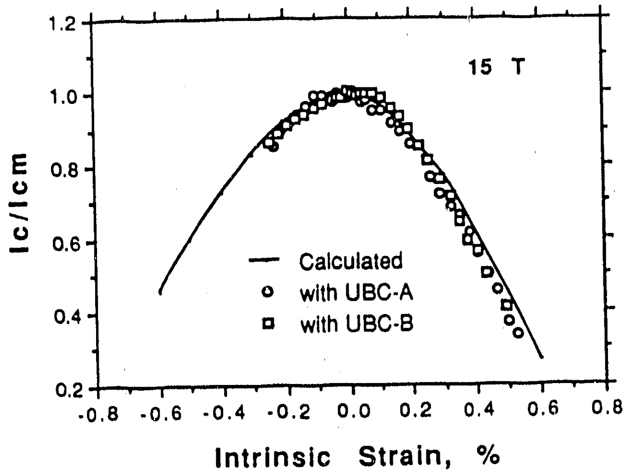

Figure 4. Critical current as a function of longitudinal strain for wires with under-barrier copper. Data is shown for two specimens (A&B). The solid line is a fit to calculated values of the strain dependence. The calculated strain dependence was obtained using the parameters in Table 2.

Table 2. Parameters used with equation 1 to calculate the critical current as a function of field and applied strain

	w / UBC	w/o UBC
B_{c20m} (T)	27.5	27.5
T_{c0m} (K)	18.3	18.3
C (AT mm^{-2})	13,500	17,500
ε (for J_c vs B)	-0.239	-0.236
a (for ε < 0)	900	900
a (for ε > 0)	1250	1250
u	1.7	1.7
w	3	3
T (K)	4.2	4.2

The critical current density of both wires as a function of field at zero applied strain are shown in Figure 3. Also shown is the predicted critical current density calculated using equation 1 and the input parameters in Table 2. The transitions observed in these wires are reasonably sharp with n values of approximately 21 at 15 T and zero applied strain.

The normalized critical current as a function of intrinsic strain is shown in Figures 4 and 5 for wires with and without UBC respectively. Also shown in these figures are calculated values of the strain dependent normalized critical current. These values were determined using the input parameters from Table 2.

The thermal precompression (average of two tests) was –0.239% and –0.236% for with and w/o UBC respectively. The irreversible strain limit (applied strain) was approximately 0.73% and 0.71%.

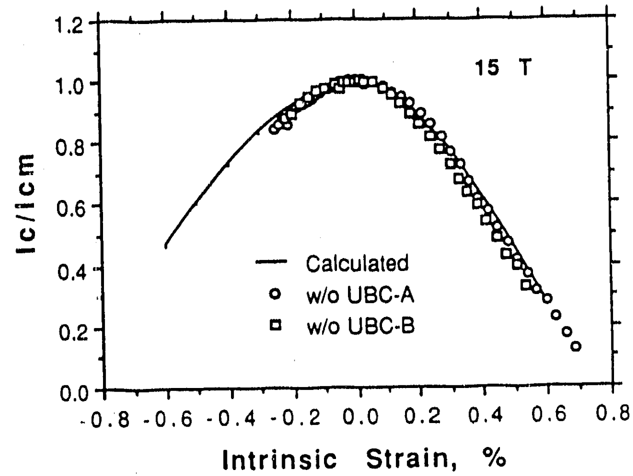

Figure 5. Critical current as a function of longitudinal strain for wires without under-barrier copper. Data is shown for two specimens (A&B). The solid line is a fit to calculated values of the strain dependence. The calculated strain dependence was obtained using the parameters in Table 2.

Discussion

An excellent fit of experimental and calculated values of normalized critical current vs strain (Figures 4 and 5) was obtained. At high positive strains (tension), calculation predicts slightly less sensitivity to strain in the wires with UBC than that obtained during testing. This is not completely unexpected as the choice of parameters, H_{c20m} and T_{c0m}, were held constant and only C allowed to vary for both wire topologies. The fit to experimental data is therefore a compromise. Subtle variations from wire topology to wire topology, such as available Sn and filament diameter, may yield small differences in H_{c20m} and T_{c0m} for the two wires. Small changes in these terms will results in large changes in the calculated fit at high compressive or tensile strains.

A reasonable fit of the of experimental J_c vs B data to the calculated values (Figure 3) is also obtained. However, significant divergence of the experimertal and calculated values are evident at low fields for both wires. This is largely reflected in the choice of H_{c20m} and T_{c0m}, whose values were constrained to obtain the the best fit to the I_c vs strain data. These values were subsequently held constant during calculation of J_c as a function of field and only the pinning/geometry factor (C) was varied.

The slight divergence of experimental and calculated data does not reduce the usefulness of the equations for predicting J_c vs B as they appear to work well within a limited range of field. However, it does suggest that the two tests, J_c vs strain and field, are not yet fully self consistent. A more detailed characterization with better control of experimental conditions is required to obtain a closer fit of the experimental and calculated data.

It should be noted that the experimental critical currents presented here are measured using a relatively low resistance criteria of $5 \times 10^{-13}\ \Omega \cdot m$. This is due to the short distance between sample voltage taps and the need to suppress the effects of spurious noise in the sample voltage and current signals. However, the large resistance criteria can lead to a slight over estimation of the critical current when compared to more sensitive criteria. Figure 6 shows the critical current of a wire with UBC at 15 T and zero applied strain as a function of resistance criteria. This data may be used to approximately scale the critical currents to a criteria of interest. It is worth noting that a resistance criteria an order of magnitude smaller than those used here (5×10^{-14} vs $5 \times 10^{-13}\ \Omega \cdot m$) yields critical currents that are approximately 15% lower.

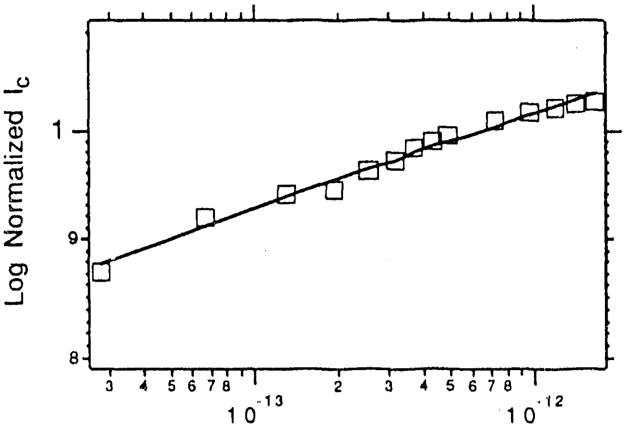

Figure 6. Approximate relation between resistance criteria and measured critical current. I_c has been normalized to the 115 A, the value obtained at a resistance criteria of $5 \times 10^{-13}\ \Omega \cdot m$ (used for most of the analyses presented here). The best fit to the normalized I_c is given by,
I_c (normalized) = 2.1 + 0.09 log (Resistance Criteria)

The overall performance of the wires examined is encouraging. The high critical current of the w/o UBC wire is excellent, providing an ample operating margin for the PoP coil. Perhaps more importantly, the high-field critical currents of the wires without under-barrier copper approach or exceed (one must account for the selection of critical current criteria) the J_c requirements established for the proposed International Thermonuclear Experimental Reactor (ITER).

Conclusions

The critical current as a function of longitudinal strain and magnetic field has been examined for two internal-Sn Nb_3Sn wires, one with and one without under-barrier copper. Precompression for both wires is similar, approximately –0.24%. The irreversible strain limit (ε_{irrev}) is approximately –.70% for both wires.

The 4 K tensile properties of both wires were nearly identical. The 0.2% offset yield strengths are approximately 205 MPa and the tensile strengths are about 640 MPa. Fracture in all specimens occurs at about 1% applied strain.

An excellent correlation between experimental and calculated J_c vs strain data was obtained. This correlation was obtained with values of H_{c20m} and T_{c0m} of 27.5 T and 18.3 K respectively. Good agreement between experimental and calculated values of J_c vs B were obtained for a limited range of fields. This fit was obtained using the same value for H_{c20m} and T_{c0m} with the pinning/geometry coefficient set to 13,500 and 17,500 for wires with and without UBC respectively.

The high field critical current of wires without the under-barrier copper is excellent. The wire is suitable for the PoP coil and appears to meet the critical current requirements established for ITER.

Acknowledgments

This work was performed under the auspices of the U.S. Department of Energy by the Lawrence Livermore National Laboratory under Contract W-7405-Eng-48.

References

1. M.J. Strum, L.T. Summers, and J.R. Miller, "Ductility enhancement in unreacted internal-Sn Nb_3Sn through low-temperature anneals," *IEEE Trans. Mag.*, V. 25, No. 2, 2208, 1989.

2. L.T. Summers, M.J. Strum, and J.R. Miller, "The characterization of Nb_3Sn superconductors for use in magnets of 19 T and greater," *Adv. Cryo. Eng.*, V. 36A, 77, 1990.

3. D.P. Hampshire, H. Jones, and E.W.J. Mitchell, "An in depth characterization of $(NbTa)_3$ Sn filamentary superconductor," *IEEE Trans. Mag.*, V. MAG-21, 289, 1985.

4. J.W. Ekin, "Strain scaling law for flux pinning in practical superconductors. Part 1: Basic relationships and application to Nb_3Sn conductors," *Cryogenics*, V. 20, 611, 1980.

5. L.T. Summers, M.W. Guinan, J.R. Miller, and P.A. Hahn, "A Model for the Prediction of Nb_3Sn Critical Current as a Function of Field, Temperature, Strain, and Radiation Damage," to be presented at the Applied Superconductivity Conference, Snowmass, CO, 1990.

- END -

DATE FILMED

11 / 16 / 90